Alagab, Samir, Tennakoon, Sarath and Gould, Chris ORCID: 0000-0002-8433-0546 (2018) Comparison of Single-stage and Multi-stage Marx DC-DC converters for HVDC application. In: 2018 53rd International Universities Power Engineering Conference (UPEC). IEEE, Glasgow, UK. ISBN 9781538629116

Official URL: https://doi.org/10.1109/UPEC.2018.8541990
DOI: http://dx.doi.org/10.1109/UPEC.2018.8541990
EPrint URI: https://eprints.glos.ac.uk/id/eprint/11639

Comparison of Single-stage and Multi-stage Marx DC-DC converters for HVDC application

Samir Milad Alagab, Sarath Tennakoon, Chris Gould.

Abstract: A high voltage DC-DC converter is a key component of future HVDC grids. This paper presents a comparison of a single-stage and multi-stage converter. Both topologies are based on the Marx principle where charged capacitors are charged in parallel and discharged in series to achieve the voltage transformation. Detailed models of both converter topologies at 50 MW, 6kV/72kV are designed and simulated using Matlab/Simulink package software.

Keywords: DC-DC converter, HVDC, IGBT, soft switching.

1. Introduction

DC-DC converters with high power and high voltage ratio are required for High Voltage Direct Current HVDC, and to act as interfaces between the generation, transmission, and distribution voltage levels [1]. There are several topologies that have been proposed in literature for HVDC DC-DC converters [2],[3],[4],[5],[6]. Most of these topologies propose to use a high-frequency transformer. However, the weight of the heavy electrical components, such as the transformer, and their physical volume, create serious issues for HVDC and are important factors in offshore wind farms. Intuitively, the Marx converter will be the most attractive and suitable configuration for HVDC applications because it avoids the use of transformers, and is lower in weight and size than alternative converter topologies.

Parastar and Gandomkar [12],[13] presented a multilevel DC-DC converter to achieve a high-gain ratio for offshore wind farms. The presence of this converter topology increases the number of conversion stages, resulting in a large number of passive components and active switches, which adds up to the system power losses and cost. Consequently, transformer less-based systems have been targeted in order to improve the wind turbine construction and maintenance requirements. Switched capacitor (SC) converters based on the Marx principle are considered as an attractive topology. Converters based on the Marx principle are capable of a realizing a high voltage gain and is a suitable for HVDC application [9],[10],[11]. Maneiro and Birkel [7],[8] presented shunt HVDC tap, using this method for stepping down the transmission voltage to a lower voltage for supplying a load, such as a remote area, where there is no existing grid. However, this topology requires a large number of IGBT switches. In this paper, a comparison of the steady-state performance of two Marx converter topologies suitable for high voltage application is presented. Single stage and multistage converters developed by the authors [14, 15] are compared, and to ensure meaningful comparison, the two converters were designed for the same voltage and current ratings. Single-stage and multi-stage structures and principles of operation are explained in Section II. A comparative performance evaluation is presented in Section III. Finally, the conclusions are drawn in section IV.

2. Single Stage and Multi-Stage Conversters

Both Marx converter topologies are compared in terms of rated voltage and power. It is assumed that a single-stage DCDC converter and multi-stage DC-DC Marx converter have already reached their steady-state. For a single stage converter, the duty cycle of both converters is fixed at 50%. The IGBT switches of both converters are operated using the soft switching technique, and the switching frequency is given.

A. Single-stage DC-DC Marx Converter • Structure configuration

As shown in Fig. 1, the structure of the converter can be divided into three sections; the input section; middle section; and the output section. The input section consists of a DC voltage source V_{in}, two HV valve switches and an input diode D_{in} connected in series with an input inductor L_{in}. The middle section comprises of '*n*' number of capacitors which is set to 12 in Fig. 1, which gives a voltage transformation ratio of 1:12, diodes $D_{(1-23)}$ and a number of IGBT switches $(S_1$-$S_{22})$, $(S_{valve2}$-$S_{valve5})$. to be Depending on the voltage level in the application a number of IGBTs are required connected in series to form high voltage switches. The 12 capacitances in the middle section are indicated by C_n, where $n = (1, 12)$.

The output section consists of three components; the output inductor L_{out}; the diode D_{out}; the output capacitor C_{out}; and the load modelled by a resistor denoted by R_{Load}. The voltage transformation is done in one stage and hence the name Single Stage Converter.

• Operating Principle

Under steady-state one cycle of operation can be explained by considering two half-cycles. In the first half cycle, 12 capacitors in the middle section are charged in parallel by the input voltage V_{in}. In Fig. 2, the charging current path through the 12 capacitors, the valve switches $(S_{valave1}$- $S_{valave5})$, diodes D_{in}, $(D_1$-$D_{23})$ and input inductor L_{in} are illustrated.

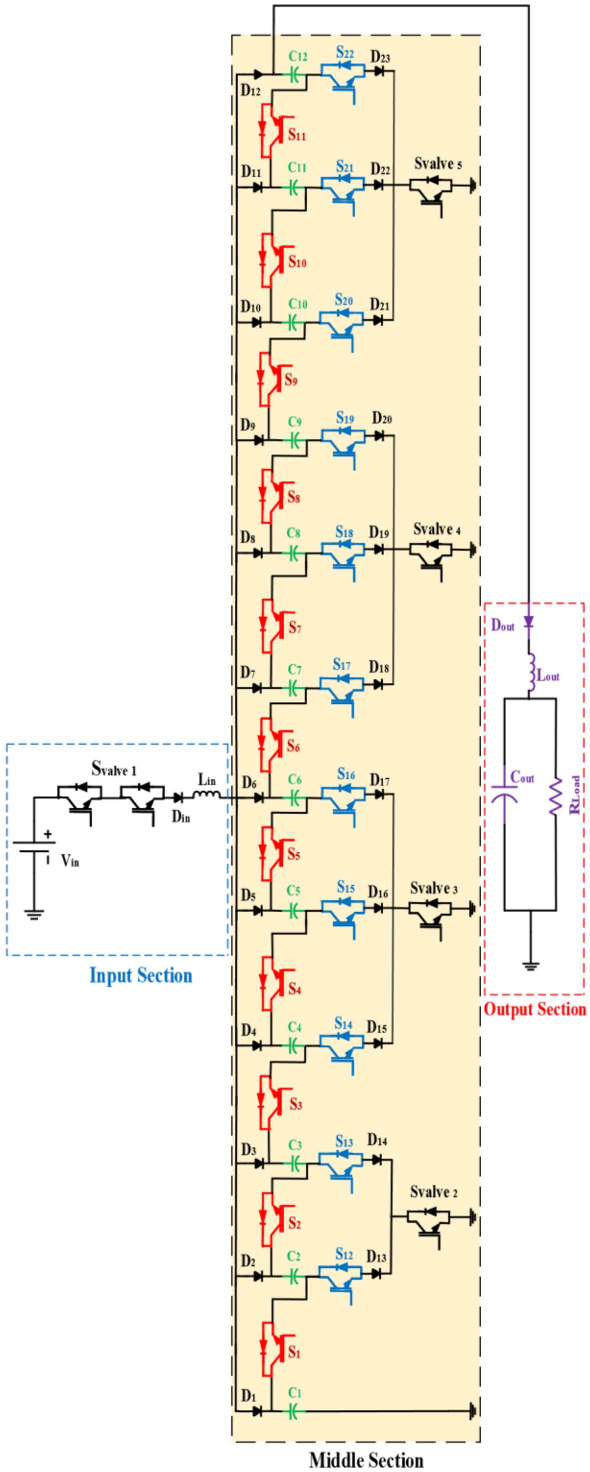

Fig. 1: Single-stage Marx converter

During the second half cycle, the 12 capacitors are discharged in series through the switches (S_1-S_{11}) to create the high voltage as depicted in Fig. 3.

The current is transferred from the middle section capacitors C_n in series to the output capacitor C_{out}, and load R_{Load} through output diode D_{out} and output inductor L_{out}. The resonance frequency of the converter is chosen to line up with the switching frequency to enable soft switching.

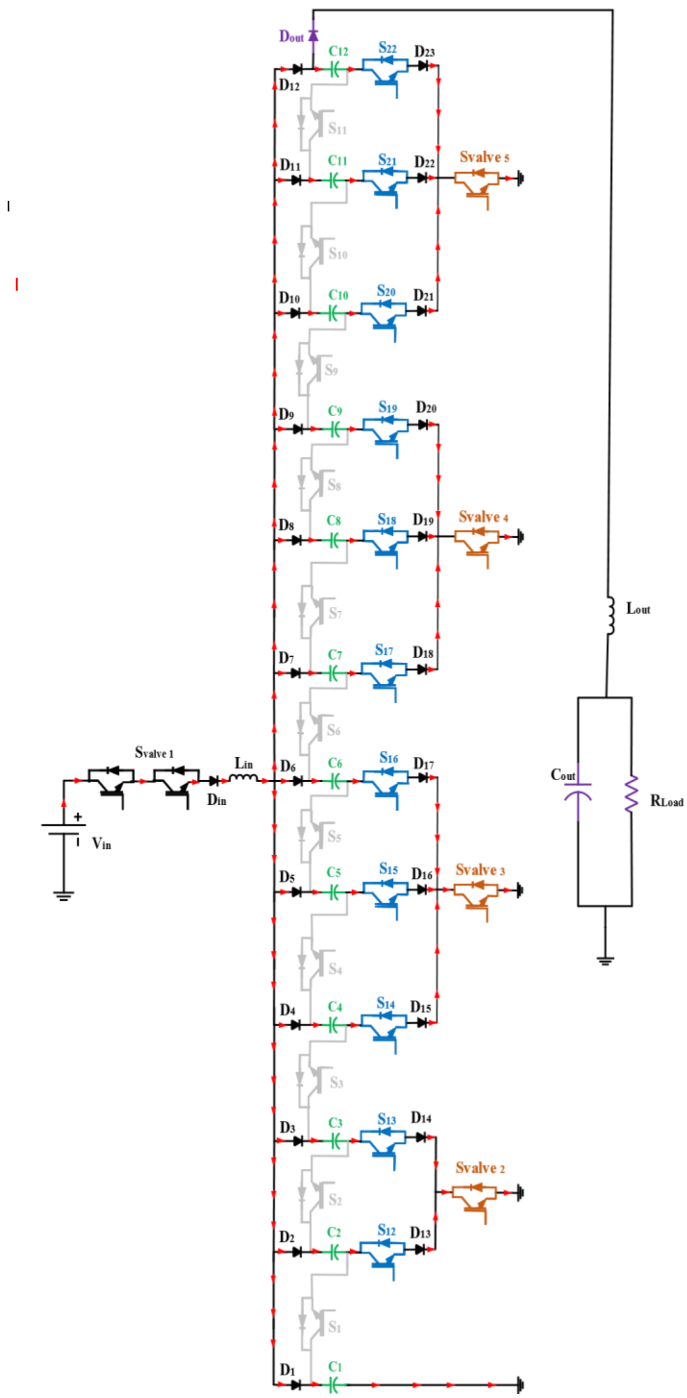

Fig. 2: First half-cycle configuration

B. Multi-stage DC-DC Marx Converter • Structure

This converter shown in Fig. 4 comprises three sections. The input and the output sections are identical to those in the single stage converter. The middle section consists of three stages rather than one stage. The number of capacitors in stages 1,2 and 3 are set to 2, 3 and 2 respectively to create the voltage gain of 2x3x2=12 as shown in Fig. 4.

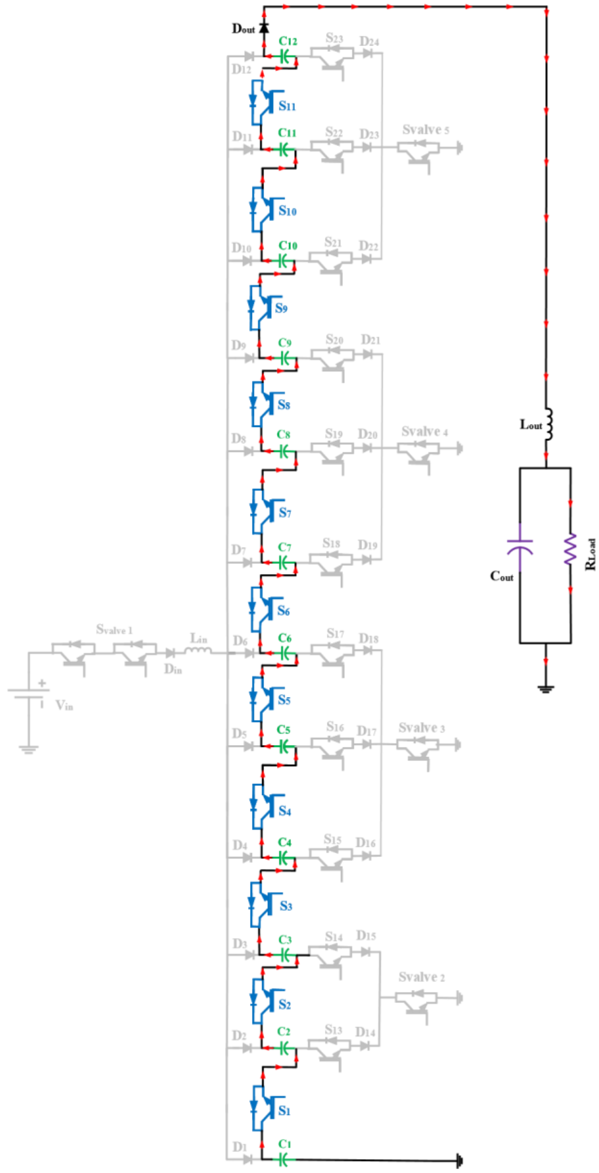

Fig. 3: Second half cycle configuration

- ***Operating Principle***

Basically, the IGBTs are switched so that the charges in capacitors are pumped from the first stage to the second stage and to the third stage sequentially, resulting in a high voltage at the converter output. The switching of the multi-stage converter is listed in Table I.

Steady state operation is considered and therefore in order to aid the explanation, it is assumed that the capacitors C_3, C_4, and C_5 in the middle stage are each charged to $2V_{in}$.

During the first half-cycle, the switch S_{valve1} is ON and the capacitors in stage 1 are charged in parallel by input voltage V_{in}, and through diode D_1, and inductor L_1. The charge on the capacitors in stage 2 discharge in series into the capacitors in stage 3 in parallel, and through inductor L_3 and diode D_7 as shown in Fig. 5.

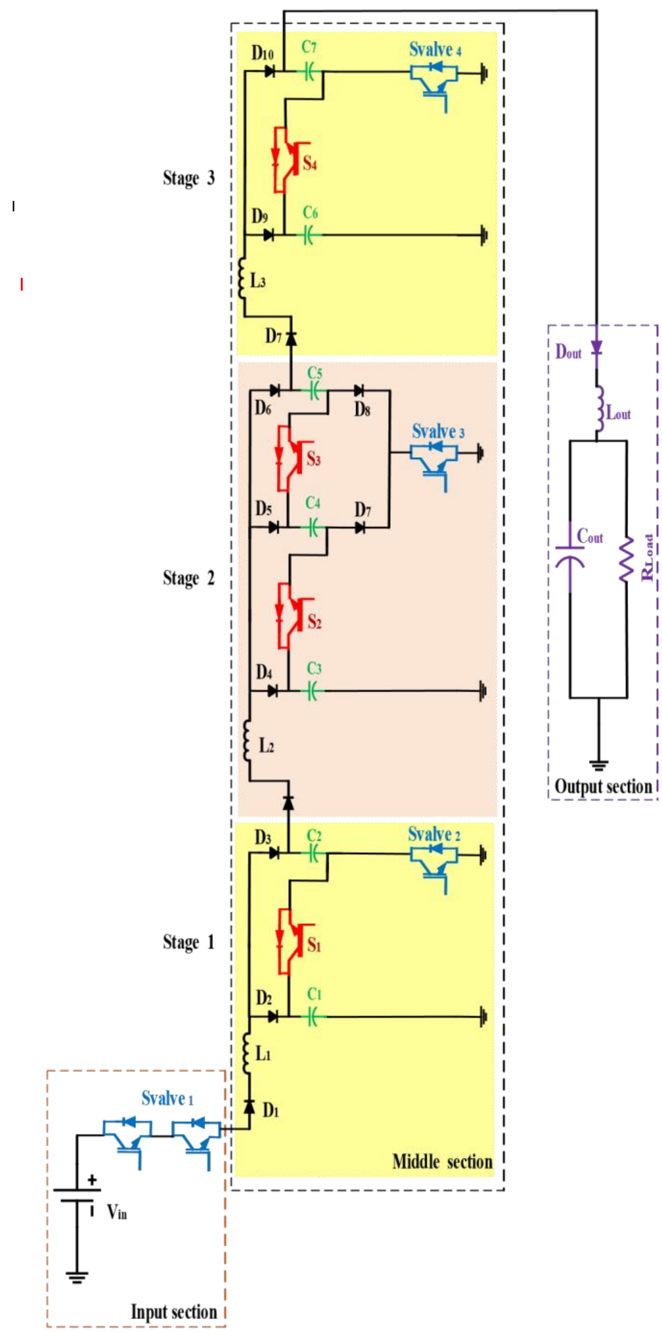

Fig. 4: Multi-stage Marx converter

TABLE I. IGBT SWITCHING LOGIC FOR THE MULTI-STAGE CONVERTER

Switches	$S_{Valve\,1}$	$S_{Valve\,2}$	$S_{Valve\,3}$	$S_{Valve\,4}$	S_1	S_2	S_3	S_4
First halfcycle	1	1	0	1	0	1	1	0
Second halfcycle	0	0	1	0	1	0	0	1

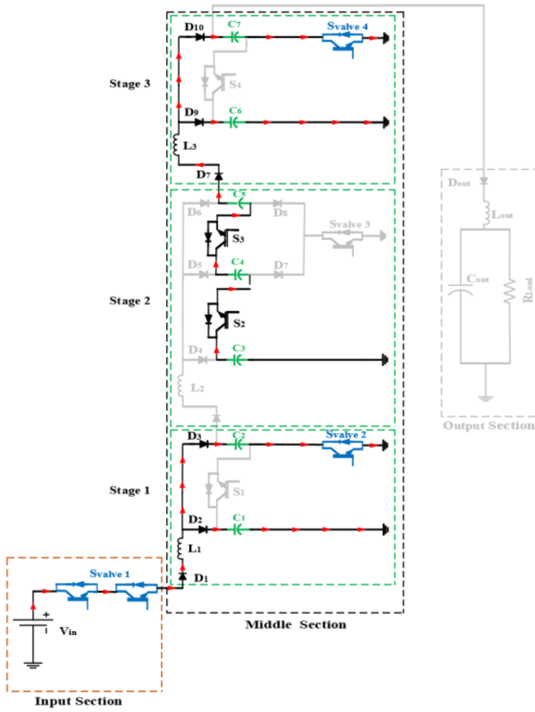

Fig. 5: First half-cycle configuration

In the second half-cycle, the device switching is the complement of the switching in the first half-cycle as depicted in Table I. The capacitors in stages 1 and 3 are in series, and the capacitors in stage 2 are in parallel, as shown in Fig. 6. The charging currents flow through inductor L_2 in stage 2 and L_{out} in the output section. Meanwhile, there is no current in the inductors L_1 and L_3. Hence, the capacitors in the middle section in stage 1 and 3 are discharged, and the capacitors in stage 2 are charged.

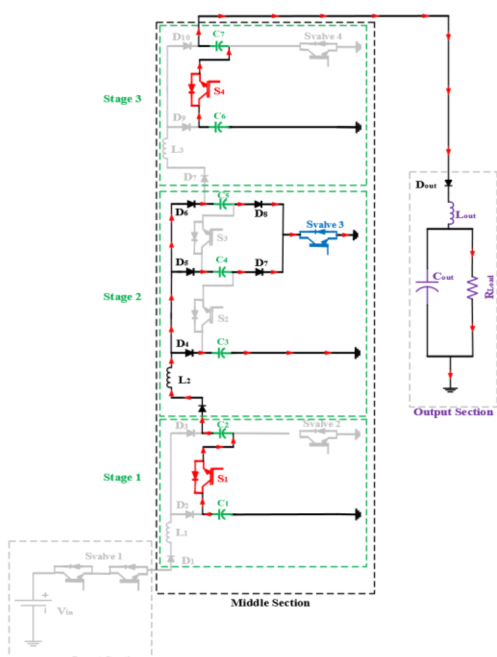

Fig. 6: Second half-cycle configuration

Continuous charging and discharging by repeated switching causes transfer of charge from the input section to the output section to supply the load R_{Load}, resulting in a voltage gain of 12. The diodes $(D_1$-$D_{10})$ which are in series with the capacitors and inductors ensure unidirectional current transfer. The output capacitor in the output section C_{out} serves as a charge storage for continuous delivery, and this capacitor has to be designed for a ripple voltage in the load.

3. Comparative Performance Evaluation

The voltage and power ratings of the converters are set to 6kV/72kV, 50MW. The switching frequency F_S = 2kHz is used with a fixed duty cycle of 50%. The load resistance was calculated using the power rating of 50 MW and the output voltage of 72kV. Both converters are simulated in the Matlab/Simulink software package. The waveforms of input and output inductor currents of both converters are shown in Fig. 7. The resonant inductor current in a single stage converter increases to a peak current of 42.3 kA.

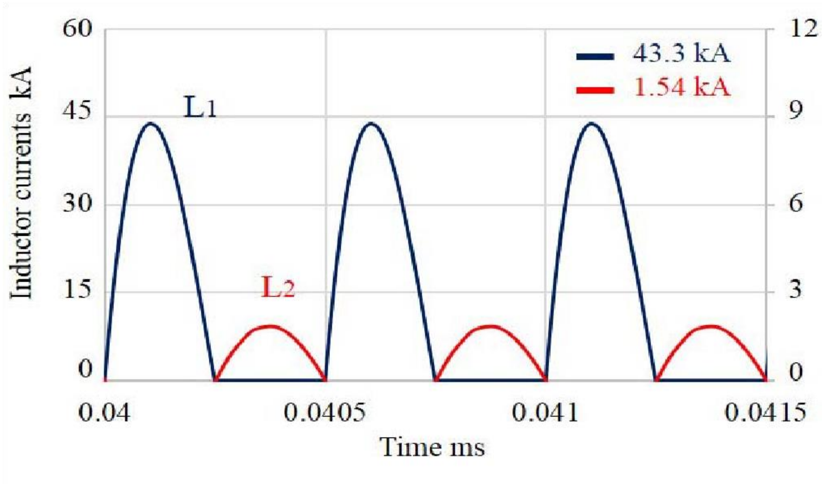

a)

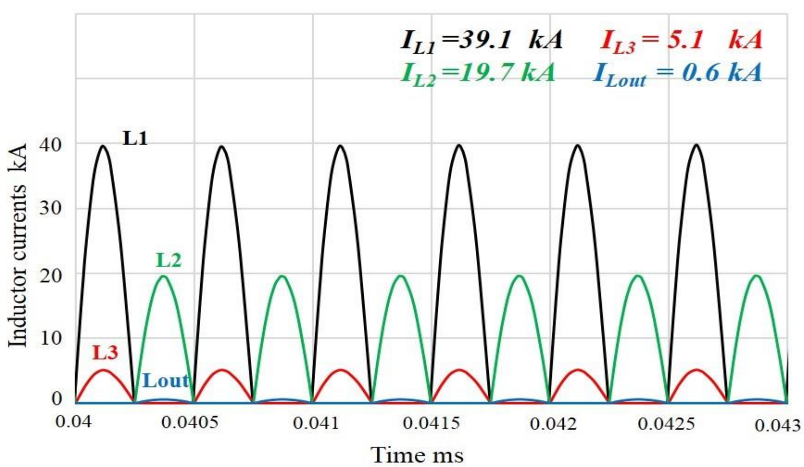

b)

Fig. 7: Inductor current waveforms: a) A single stage converter, b) Multistage converter

Fig. 7 clearly shows the effect of soft-witching, where current zeros resulting from the L-C oscillations lead to a reduction in switching losses. The resonating inductor current of the multi-stage converter increases to a peak of around 39kA in 250μs, while the resonant inductor current of the single stage converter increases to a peak of around 43.3kA. As shown in [16], the surge current capability of the ABB IGBT switch 5SNA 1200G450300 is 80kA in 100 μs, and 14kA in 10ms.

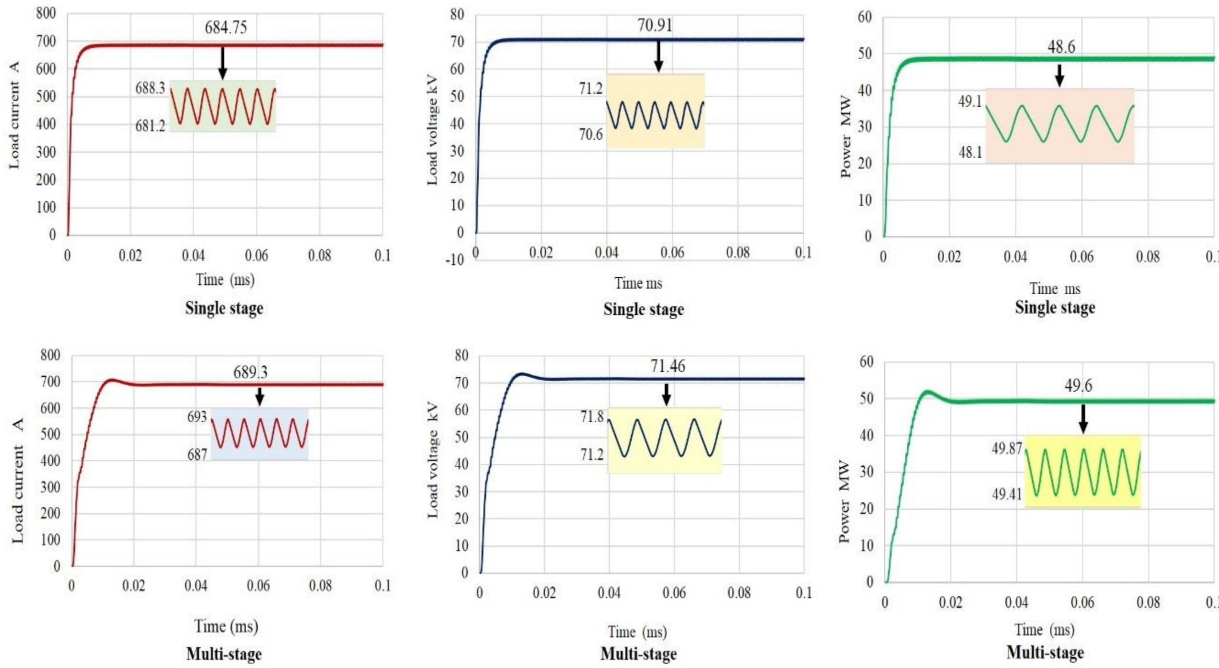

Fig. 8: Load voltage, Load current and load power waveforms both of converters

A quantitative comparison was carried out using data from the output results by Matlab/Simulink simulation. Both singlestage and multi-stage converters are evaluated and compared in terms of the power device count, to highlight its advantages for high-voltage applications. As mentioned before, both converter topologies operate under the same DC-DC Marx converter principle; hence, the comparison is made for the same voltage gain, same input voltage, same power rating, same load, same soft switching technique, and same switching frequency. Fig. 8, shows the simulation results of a single stage and a multi-stage converter. The DC gain of a single stage and multi-stage converter is 11.81 and 11.92 respectively, and have been compared with the theoretical gain of 12.

The output voltage, current, and power of the converter should be 72KV/ 694.5 A, 50MW as designed. It can be seen that both circuit output voltages are 70.91kV and 71.46kV respectively, which is very close to the design specification of 72kV. Fig. 8 shows that the output voltage in the multi-stage converter is higher than that of the single-stage converter, but both topologies perform equally well. Comparing with other HV DC-DC topologies that have a high gain ratio, they do not demonstrate a similar reduction in semiconductor components in the same application, perhaps because this has not been a focus area for the designer. Also, the peak load current of both converters is 684.75 A and 689.3 A, which is very close to the design value of 694.5 A. In addition, the load power of both converters as shown in Fig. 8 is 48.6MW and 49.6MW.

For both configurations, IGBT switches are comprised of several series-connected power devices to withstand the rated voltage.

Fig. 9 shows the active and passive component count comparison with a different gain voltage between both of the converter topologies. For both configurations, IGBT switches and diodes are comprised of several series-connected power switches to withstand the rated voltage. Currently, the high voltage has a maximum blocking voltage rated up to 6.5 kV 600A, but the ratings of the IGBT considered for this study is 4.5 kV and 1200 A. An inspection of the characteristics of the IGBT 5SNA 1200G450300, shows that this is feasible

[16]. The required number of IGBT switches and diodes is mainly determined by peak current and peak voltage. The number of capacitors is calculated based on the required voltage rating and capacitance. The input and output sections of both converter topologies require the same number of active switches.

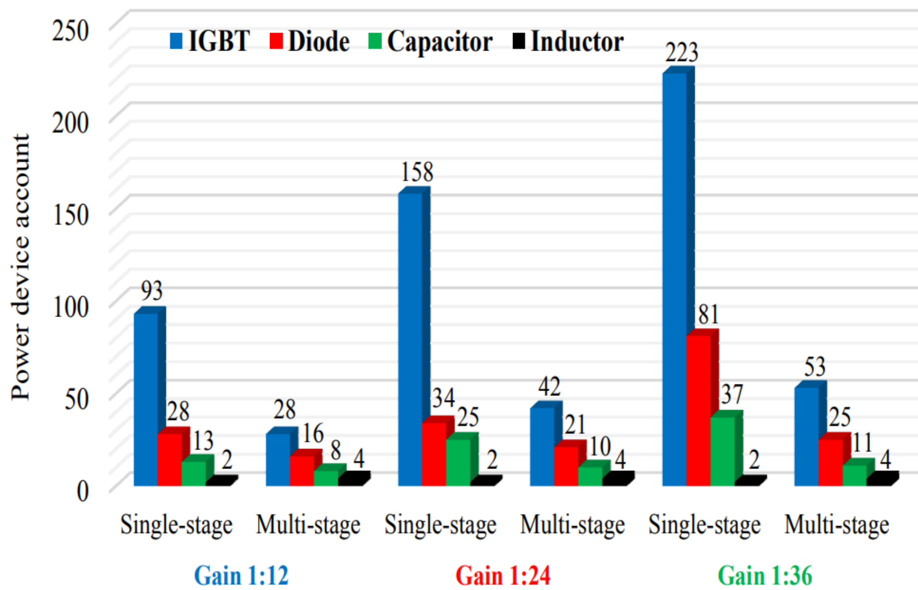

Fig. 9: Components count for DC-DC converter topologies comparisons between single-stage and multi-stage converters

As shown in Fig. 9, the comparison of designs includes three different voltage gains of 1:12, 1:24, and 1:36. The number of IGBT switches and capacitors in multi-stages is reduced when compared with a single-stage component, except for the inductor count which increases by a fixed small margin of only 2, and can be increased and depends on the number of stages in the middle section of the multi-stage converter.

In the multi-stage topology, the increase of the active switches (24%) depends on the voltage gain, while in the single stage topology there is a large increase of the active and passive components of 69%. The reduction in the component count in the multi-stage converter leads to a reduction of weight, cost, and complexity.

4. Conclusions

In this paper, two DC-DC converters based on the Marx principal for HVDC applications are compared with each other. The principles of operation of both DC-DC converter concepts are described and validated by computer simulations. The simulation findings show that the single-stage converter requires a large number of switching devices and passive components when compared with the multi-stage converter. Therefore, the physical volume and weight of a single-stage converter is higher than a multi-stage converter. Although both topologies achieve the required voltage gain of 12, the simulation results demonstrate that the voltage drop in a single-stage converter is more than the voltage drop in the multi-stage converter. Finally, it can be concluded that both single-stage and multi-stage converters are suitable and recommended for HVDC application.

REFERENCES

[1] S. M. Alagab, S. Tennakoon, and C. Gould, “Review of wind farm power collection schemes,” *Proc. Univ. Power Eng. Conf.*, vol. 2015–Novem, 2015.

[2] M. Barrenetxea, I. Baraia, I. Larrazabal, and I. Zubimendi, “Design of a Novel Modular Energy Conversion Scheme for DC Offshore Wind Farms,” 2015.

[3] M. Moonem, C. Pechacek, R. Hernandez, and H. Krishnaswami, “Analysis of a Multilevel Dual Active Bridge (ML-DAB) DC-DC Converter Using Symmetric Modulation,” *Electronics*, vol. 4, no. 2, pp. 239–260, Apr. 2015.

[4] S. Liu, L. Shi, and Z. Chen, “Improved zero-voltage-switching pulse width modulation full bridge converter with self-regulating auxiliary current,” *IET Power Electron.*, vol. 6, no. 2, pp. 287–296, 2013.

[5] Zakis, Janis, Dmitri Vinnikov, and Ivars Rankis. "Steady state analysis of the galvanically isolated DC/DC converter with a commutating LC filter." Industrial Technology (ICIT), *2012 IEEE International Conference on. IEEE, 2012.*

[6] Y. A. N. Zhou, Y. Lian, G. P. Adam, and S. J. Finney, “ DC / DC Converter for Offshore Dc Collection Grid,” pp. 7–11.

[7] J. Maneiro, S. Tennakoon, and C. Barker, “Scalable shunt connected HVDC tap using the DC transformer concept,” *2014 16th Eur. Conf. Power Electron. Appl. EPE-ECCE Eur. 2014*, pp. 6–8, 2014.

[8] A. Birkel and M. M. Bakran, “Comparison of shunt connected tapping concepts in HVDC transmission systems,” *2016 18th Eur. Conf. Power Electron. Appl. EPE 2016 ECCE Eur.*, 2016.

[9] A. Parastar, A. Gandomkar, M. Jin, and J. K. Seok, “High power solid-state step-up resonant Marx modulator with continuous output current for offshore wind energy systems,” *2013 IEEE Energy Convers. Congr. Expo. ECCE 2013*, pp. 1709–1716, 2013.

[10] P. W. Lehn, B.-T. Ooi, and E. Veilleux, “Marx dc–dc converter for high-power application,” *IET Power Electron.*, vol. 6, no. April, pp. 1733–1741, 2013.

[11] E. Veilleux and B. T. Ooi, “Marx-dc-dc converter for connecting offshore wind farms to multiterminal HVDC,” *IEEE Power Energy Soc. Gen. Meet.*, pp. 1–5, 2013.

[12] A. Parastar, A. Gandomkar, and J. Seok, “High-Efficiency Multilevel Flying-Capacitor Renewable Energy Systems,” vol. 62, no. 12, pp. 7620–7630, 2015.

[13] A. Gandomkar, S. Member, A. Parastar, S. Member, J. Seok, and S. Member, “High-Power Multilevel Step-Up DC / DC Converter for Offshore Wind Energy Systems,” vol. 46, no. c, 2016.

[14] S. M. Alagab, S. B. Tennakoon, and C. A. Gould, “A Compact DCDC Converter for Offshore Wind Farm Application,” *Renew. Energy Power Qual. J.*, vol. 1, no. 15, pp. 529–533, 2017.

[15] S. M. Alagab, S. B. Tennakoon, and C. A. Gould, “High Voltage Cascaded Step-Up DC-DC Marx Converter for Offshore Wind Energy Systems,” *EPE 2017 - assigned jointly to Eur. Power Electron. Drives Assoc. Inst. Electr. Electron. Eng.*, no. Mmc, pp. 1–10, 2017.

[16] ABB Switzerland Ltd., “Surge currents for IGBT diodes, Application Note 5SYA 2058-02,” 2014.